Article

Biological studies and target-engagement of the 2-C-methyl-D-erythritol 4-phosphate cytidylyltransferase (IspD)-targeting antimalarial agent (1R,3S)-MMV008138 and analogs

Maryam Ghavami, Emilio Fernando Merino, ZhongKe Yao, Rubayet Elahi, Morgan Simpson, Maria Fernandez-Murga, Joshua Hayden Butler, Michael Casasanta, Priscilla Krai, Maxim Totrov, Daniel J. Slade, Paul R. Carlier, and Maria Belen Cassera

ACS Infect. Dis., **Just Accepted Manuscript** • DOI: 10.1021/acsinfecdis.7b00159 • Publication Date (Web): 26 Oct 2017

Biological studies and target-engagement of the 2-*C*-methyl-D-erythritol 4-phosphate cytidylyltransferase (IspD)-targeting antimalarial agent (1*R*,3*S*)-MMV008138 and analogs

Maryam Ghavami,[†] Emilio F. Merino,[‡,§] Zhong-Ke Yao,[†] Rubayet Elahi,[‡] Morgan E. Simpson,[‡] Maria L. Fernández-Murga,[‡] Joshua H. Butler,[§] Michael A. Casasanta,[‡] Priscilla M. Krai,[‡] Maxim M. Totrov,[¶] Daniel J. Slade,[‡] Paul R. Carlier,[*,†] and Maria Belen Cassera[*,‡,§]

[†]Department of Chemistry and Virginia Tech Center for Drug Discovery, Hahn Hall South, 800 West Campus Drive, Virginia Tech, Blacksburg, Virginia 24061, United States

[‡]Department of Biochemistry and Virginia Tech Center for Drug Discovery, Engel Hall, 340 West Campus Drive, Virginia Tech, Blacksburg, Virginia 24061, United States

[§]Department of Biochemistry and Molecular Biology, and Center for Tropical and Emerging Global Diseases (CTEGD), 120 Green St., University of Georgia, Athens, Georgia 30602, United States

[¶]Molsoft LLC, 11199 Sorrento Valley Road, San Diego, California 92121, United States

*Correspondence:

Maria Belen Cassera, maria.cassera@uga.edu, Tel. 706-542-5192, FAX 706-542-1738

Paul R. Carlier, pcarlier@vt.edu, Tel. 540-231-9219, FAX 540-231-3255

Malaria continues to be one of the deadliest diseases worldwide, and the emergence of drug resistance parasites is a constant threat. *Plasmodium* parasites utilize the methylerythritol phosphate (MEP) pathway to synthesize isopentenyl pyrophosphate (IPP) and dimethylallyl pyrophosphate (DMAPP), which are essential for parasite growth. Previously, we and others identified that the Malaria Box compound MMV008138 targets the apicoplast, and that parasite growth inhibition by this compound can be reversed by supplementation of IPP. Further work has revealed that MMV008138 targets the enzyme IspD in the MEP pathway, which converts MEP and CTP to cytidine diphosphate methylerythritol (CDP-ME) and pyrophosphate. In this work, we sought to gain insight into the structure-activity relationships by probing the ability of MMV008138 analogs to inhibit *Pf*IspD recombinant enzyme. Here, we report *Pf*IspD inhibition data for fosmidomycin (FOS) and 19 previously disclosed analogs, and report parasite growth and *Pf*IspD inhibition data for 27 new analogs of MMV008138. In addition, we show that MMV008138 does not target the recently characterized human IspD, reinforcing MMV008138 as a prototype of a new class of species-selective IspD-targeting antimalarial agents.

Key words: *Plasmodium, malaria, MEP pathway, MMV008138, IspD, structure-activity studies*

Human malaria is caused by five species of *Plasmodium*. Around 250 million cases of malaria occur every year with 95% of the infections caused by *Plasmodium falciparum* and *Plasmodium vivax*.[1] Malaria continues to be one of the deadliest diseases worldwide, and the continued emergence of drug resistance is a constant threat. Therefore, efforts to identify and characterize new leads for development of antimalarial drugs with different mechanisms of action are still needed. In order to catalyze the development of new antimalarials, the Medicines for Malaria Venture (MMV) and SCYNEXIS assembled the Malaria Box,[2] an open access library composed of 400 compounds originally identified by phenotypic screening of nearly 6,000,000 compounds from the research libraries of Saint Jude Children's Research Hospital, Novartis, and GlaxoSmithKline.[3] Over 290 assays had been performed to screen the Malaria Box and substantial information about these compounds is now available.[4]

Malaria parasites contain a vestigial plastid called the apicoplast, which performs vital functions such as the biosynthesis of isoprenoid precursors, fatty acids, and part of the heme.[5-6] *Plasmodium* parasites utilize the methylerythritol phosphate (MEP) pathway to synthesize isopentenyl pyrophosphate (IPP) and dimethylallyl pyrophosphate (DMAPP), which are essential for parasite growth.[7-8] This pathway is absent in humans, who rely on the mevalonate pathway instead. Recently, it has been suggested that the MEP pathway and the biosynthesis of the isoprenoid precursors IPP and DMAPP represent the sole essential function of this organelle during asexual intraerythrocytic development of the parasites[9] as well as during gametocytogenesis.[10] The strongest support for this proposal stems from the observation that both loss of the apicoplast function as well as loss of the organelle can be chemically rescued by supplementing the growth medium with IPP. Therefore, the growth inhibitory effect of drugs that directly target biosynthesis of isoprenoid precursors or indirectly disrupt their biosynthesis by interfering with processes essential for apicoplast biogenesis, such as apicoplast DNA replication, transcription, and protein translation, may be reverted by IPP supplementation.[9] As a result, the reversal of growth inhibition by IPP supplementation can be used as a phenotypic

screening diagnostic to identify compounds that target the apicoplast, thus, identifying their mechanism of action and narrowing their potential molecular targets.[9] Previously, we identified the drug-like Malaria Box compound MMV008138 (Figure 1) using this method, and proposed that the molecular target may be within the MEP pathway, especially because we noted that MMV008138 did not present a delayed death phenotype and the apicoplast was not lost in the presence of IPP, similar to fosmidomycin (FOS).[11] Further analyses revealed that the active stereoisomer of this molecule is (1*R*,3*S*)-configured,[12-13] and that its MEP pathway target is the cytidylyltransferase IspD (E.C.2.7.7.60) which converts 2-*C*-methyl-D-erythritol 4-phosphate (MEP) and CTP to cytidine diphosphate methylerythritol (CDP-ME) and pyrophosphate.[12, 14]

One of the most striking features of (1*R*,3*S*)-MMV008138 (henceforth **1a,** Scheme 1) is its species-selectivity toward the malarial IspD.[12, 14] Though **1a** was reported to inhibit *P. falciparum* IspD with K_i values in the 7-13 nM range, it did not inhibit *Arabidopsis thaliania*, *Mycobacterium tuberculosis*, or *Escherichia coli* IspDs at concentrations up to 10 μM.[12, 14] This *E. coli* IspD (*Ec*IspD) insensitivity is especially important since the MEP pathway is present in the human microbiome.[15] Therefore, unlike antibiotics such as doxycycline (DOX) that kill malaria parasites by interfering with apicoplast's genome expression,[16] or FOS that inhibits 1-deoxy-D-xylulose 5-phosphate reductoisomerase (DXR) in the MEP pathway also affecting the gut microbiome,[8, 17-19] compound **1a** may not affect beneficial gut bacteria. Moreover, doxycycline is used for prophylaxis in endemic areas with multidrug-resistance and in combination therapies; however, it is not recommended for pregnant women and children under the age of 8.[20] Therefore, antimicrobial agents that are parasite-specific are ideally suited for the development of malaria chemopreventive agents that are not toxic to pregnant women and children and do not impact the human intestinal microbiome. Indeed, we previously confirmed that **1a** had no effect on *E. coli* growth at concentrations up to 500 μM.[13]

Subsequent to our discovery of **1a** as a MEP-pathway inhibitor,[11] we prepared 34 close structural analogs designed to probe *P. falciparum* growth inhibition structure-activity

relationships (SAR).[13] We determined that in addition to (1*R*,3*S*)-configuration, potent growth inhibition required 2,4-disubstitution of the D-ring, featuring at least one electron-withdrawing substituent. For example, whereas **1a** inhibited *P. falciparu*m (Dd2 strain) growth with an IC_{50} value of 250 ± 50 nM, neither **1b** (bearing an unsubstituted phenyl ring) nor **1u** (bearing 2',4'-dimethyl substitution) inhibited *P. falciparum* growth at 10,000 nM (Figure 1). However, 2'-chloro substituted analog **1c** showed weak growth inhibition, and **1e** (2'-chloro-4'-methyl substituted) nearly recapitulated the potency of **1a**. The carboxy substituent at C3 of the C ring also proved to be essential; replacement with CO_2Me (**3a**) or H ((±)-**11a**) abrogated growth inhibition potency. However, weak growth inhibition was restored with the first amide analog **6a**, and methyl amide derivative **7a** proved equipotent to **1a**.

In the present work, we sought to gain insight into these structure-activity relationships by probing the ability of these compounds and new analogs to inhibit *Pf*IspD recombinant enzyme, the proposed parasite target of **1a**. In this paper, we report *Pf*IspD inhibition data for FOS and 19 previously disclosed analogs, and report growth inhibition and *Pf*IspD inhibition data for 27 new analogs of **1a**. As we will show below, these analogs show an excellent correlation between *P. falciparum* Dd2 strain growth inhibition and *Pf*IspD inhibition, confirming the proposed antimalarial mode of action. In addition, we expanded the biological studies to assess cytotoxicity and stage specificity profile of **1a**.

RESULTS AND DISCUSSION

Structure-activity relationships. We first measured the kinetic parameters of recombinant IspD (K_m^{MEP} = 12.0 ± 2.5 μM, k_{cat}^{MEP} = 7.6 ± 0.6 s^{-1}, K_m^{CTP} = 9.3 ± 2.5 μM, k_{cat}^{CTP} = 11.7 ± 1.2 s^{-1}) using PhosphoWorks™ Fluorimetric Pyrophosphate Assay Kit (AAT Bioquest®, Inc.) which directly measures pyrophosphate (PP_i) released from the IspD-catalyzed reaction (MEP + CTP → CDP-ME + PP_i,) (see Supporting Information, Figure S2). Previously reported kinetic parameters of the substrate CTP for this construct were K_m^{CTP} = 59 μM and k_{cat}^{CTP} = 0.43 s^{-1}.[14] In

addition, Wu and colleagues reported kinetic parameters of the substrate MEP K_m^{MEP} = 61 μM, k_{cat}^{MEP} = 0.16 s^{-1} using a histidine- and maltose binding protein-tagged *Pf*IspD protein.[12] However, in both cases different detection assays (EnzChek Phosphate and Pyrophosphate Assay Kits) were used to indirectly measure release of pyrophosphate through its subsequent conversion to phosphate. After the kinetic parameters were determined, we first studied the inhibitory properties of **1a**, its three diastereomers **5a**, *ent*-**1a**, *ent*-**5a**, and the antimalarial FOS (Table 1). As was first reported by Wu et al,[12] we confirmed that among the 4 stereoisomers of MMV008138, (1*R*,3*S*)-configured **1a** is the most potent inhibitor of *Pf*IspD (IC_{50} = 44 ± 15 nM). Thus, the stereochemical dependence of *P. falciparum* growth inhibition potency correlates very well with *Pf*IspD target engagement. Furthermore, as expected, the IspC (DXR)-targeting antimalarial FOS is a poor inhibitor of *Pf*IspD (~4% inhibition at 10 μM). We would also note that the toxicological selectivity of **1a** is much higher than that of FOS: whereas **1a** has no effect on *E. coli* growth at 2,000-fold of its *P. falciparum* growth inhibition IC_{50} value, FOS shows an *E. coli* MIC only 14-fold higher than its *P. falciparum* growth inhibition IC_{50} value. This toxicological selectivity is expected, since **1a** does not engage *Ec*IspD.[12, 14] Interestingly, while (1*S*,3*R*)-configured *ent*-**1a** and (1*S*,3*S*)-configured **5a** have no effect on *E. coli* growth at 250 μM and 125 μM, (1*R*,3*R*)-configured *ent*-**5a** inhibited 18 ± 6 % of *E. coli* growth at 250 μM.

As alluded to above, previously we observed a very tight D-ring SAR for analogs of **1a**; only analogs bearing at least one sterically small, electron-withdrawing substituent at 2' and/or 4' were potent *P. falciparum* growth inhibitors (e.g. **1e-g**).[13] To further test this hypothesis, 17 new acid analogs of **1a** were prepared and compared to previously synthesized analogs (Table 2). As can be seen, *P. falciparum* growth inhibition potency is retained in compounds **1h**-**l** that feature single replacement of the Cl atoms of **1a** with F (**1h**, **i**), Br (**1j**, **k**), or both Cl atoms of **1a** with Br (**1l**). Within experimental error, compounds **1j** and **1k** are equipotent to **1a**, but compounds featuring 2'-I,4'-F, 2'-F,4'-I, or 2'-Br,4'-I substitution (**1m-o**) were less potent growth

inhibitors. Nevertheless, compounds **1e**-**n** all showed full rescue upon addition of 200 μM IPP, confirming their action as MEP pathway inhibitors. However, replacement of one of the Cl atoms of **1a** with OMe, OH or CO_2H (**1p**-**s**) significantly reduces growth inhibition potency. Compounds featuring very large electron-withdrawing groups (**1t**) or electron-releasing substituents at 2',4' (**1u**, **1v**) are also poor *P. falciparum* growth inhibitors. A few compounds featuring 3',4'-disubstitution (**1w**, **1x**), tri- and tetra-substitution (**1y**, **1z**, **1aa**), and heterocyclic modification (**1ab**, **1ac,**) were also explored, and found to be poor *P. falciparum* growth inhibitors. Two modifications of the C-D ring junction of **1a** were explored. Compound **1ad** features the insertion of a CH_2 unit between the C and D rings of **1a**, and this modification abrogated growth inhibition. Secondly, preparation of a derivative of **1a** that featured replacement of the C1-H with methyl was attempted via a ketone Pictet-Spengler reaction with 2,4-dichlorophenyl methyl ketone (vide infra). Although the expected product of this reaction could not be isolated, compounds **1ae** and **1af** were successfully prepared by ketone Pictet-Spengler reactions with 4-chlorophenyl methyl ketone and acetophenone. However, these compounds also did not inhibit growth of the parasite below 5 μM. Thus, the new compounds synthesized reinforce our earlier conclusion that potent growth inhibition by analogs of **1a** requires 2',4'-disubstitution of the D-ring, featuring at least one electron-withdrawing substituent.

The *Pf*IspD inhibition potencies of these compounds largely follow the same trend (Tables 1, 2). Unsubstituted or monosubstituted D-ring derivatives (**1b**-**1d**, IC_{50} = 510 to >5,000 nM) are weaker inhibitors than **1a** (IC_{50} = 44 ± 15 nM). Close analogs of **1a** featuring 2',4'-disubstitution with at least one small electron-withdrawing group (**1e**-**1l**) feature *Pf*IspD IC_{50} values ranging from 31 – 260 nM, consistent with their potent growth inhibition (IC_{50} = 320 – 860 nM). Note that several potent compounds (**1a**, **1e**, **1i**-**1l**) have *Pf*IspD IC_{50} values close to the nominal enzyme concentration in the assay (60 nM), and thus these values represent our current best estimates. This nominal enzyme concentration represents a practical current lower limit, based on the sensitivity of the assay (0.1 μM of PPi); if assay at lower nominal enzyme

concentration could be performed, it is possible that the measured IC_{50} values of these compounds would be lower. Therefore, differences in the measured *Pf*IspD IC_{50} values of **1a**, **1e**, and **1i**-**1l** (31 – 100 nM) may not be reflective of actual differences in target-site affinity of these compounds. Finally, as was seen for growth inhibition, replacement of the C2' and C4' Cl groups of **1a** with CF_3, Me, or OMe (**1t**-**1v**), or 3',4'-Cl_2 substitution (**1w**) significantly reduced *Pf*IspD inhibition. Thus, the antimalarial activity of D-ring analogs of **1a** appears very well correlated to the extent of their engagement with *Pf*IspD. This tight SAR suggests that the D-ring projects into a very well-defined cavity of *Pf*IspD, and is not solvent-exposed. The requirement that at least one of the substituents at C2' or C4' must be a halogen (cf. **1a** vs **1e**/**1f** vs **1u**) is curious, and could be a consequence of a number of phenomena. It is possible that halogen-bonding[21] to one or more *Pf*IspD backbone carbonyl groups contributes to affinity, as was characterized crystallographically for the 1,3-dihalobenzene moieties present in the pseudillin inhibitors of *A. thaliana* IspD.[22]

We then examined several of the carboxylic acid replacement analogs of **1a** disclosed in our earlier publication (**3a**, **6a**, **7a**, **7e**, **11a**), and six new ones (**7i**-**7k**, **8a**, **9a**, **10a,** Table 3). As mentioned earlier methyl ester (**3a**) was a poor *P. falciparum* growth inhibitor, and as expected this compound does not measurably inhibit *Pf*IspD at 1,000 nM. The 1° amide **6a** does inhibit growth of *P. falciparum* in the 1 μM range, and its potency to inhibit *Pf*IspD is similar. Methyl amides (**7a**, **7e**, **7i**-**k**) proved to be excellent replacements for the carboxylic acid group, both for growth inhibition (IC_{50} = 190 – 506 nM) and for *Pf*IspD inhibition (IC_{50} = 21 – 360 nM). With respect to growth inhibition, **7j**, **7k** are equipotent to **1a** (within error), and **7a**, **e**, **i**-**k** all show 100% rescue upon supplementation with 200 μM IPP. The methyl amides also show very weak inhibition of *E. coli* growth at 250-500 μM. Finally, the ethyl amide (**8a**), *N*,*N*-dimethyl amide (**9a**), 1° alcohol analog (**10a**) and racemic des-carboxy derivative **11a** showed poor growth and *Pf*IspD inhibition. Thus, within this limited series antimalarial activity is also well-correlated to *Pf*IspD engagement. These data and those in Table 1 show that the carboxylate group of **1a**

plays a critical role in interacting with *Pf*IspD; however, the nature of this interaction is not clear. A purely electrostatic interaction of the carboxylate of **1a** with *Pf*IspD is ruled out by the potency of methyl amide **7a.** Yet the carboxylate cannot simply serve as a hydrogen-bond acceptor, since the isosteric 1° amide **6a** does not potently engage *Pf*IspD. In any event, the carboxylate and methylamide groups of **1a** and **7a** must project into a rather constricted pocket, since ethyl amide **8a** and *N*,*N*-dimethyl amide **9a** dramatically lose potency relative to methyl amide **7a.**

***Pf*IspD inhibitor 1a is cytocidal in late trophozoite-early schizont stages but not in ring stage.** In our previous study we demonstrated that **1a** (MMV008138) targets the apicoplast, where it inhibits elongation and disturbs the mitochondrial membrane; these effects are reversed upon IPP supplementation.[11] However, the parasite's development was arrested at the early schizont stage, since DNA replication (assessed by Hoechst staining) was still observed after 40 h of treatment with 2.5 μM of **1a**.[11] Therefore, to better assess if **1a** is cytocidal and parasite stage-specific we determined the 50% lethal concentration (LC_{50}) at 72 h using highly synchronous cultures starting at ring stage and bolus incubation times ranging from 6 to 24 h. At each indicated time, **1a** was washed out and parasites were returned to culture to complete 72 h growth, at which point growth was measured by SYBR Green assay (Figure 2). In parallel, cultures were smeared and stained with Giemsa for stage assessment of **1a**-treated and control parasites at the time that **1a** was washed out. The SYBR Green assay at 72 h confirmed that parasites were able to grow similarly to untreated controls following 6 and 12 h incubation with **1a**, therefore, the LC_{50} values could not be determined. However, when incubation with **1a** was extended to the late-trophozoite/early schizont stage (18 h), the LC_{50} value was 1.20 ± 0.08 μM. When the drug incubation was extended to 24 h, the measured LC_{50} value further decreased to 0.46 ± 0.02 μM, which was very close to the measured IC_{50} value at 72 h performed simultaneously with these assays (0.35 ± 0.03 μM). The cytocidal action of **1a,** therefore,

manifests at 18-24 h, which is the time needed for parasites to progress from ring to late trophozoite/early schizont stage. This transition marks the period of highest metabolic activity of the MEP pathway, as discussed below (Figure 3). The absence of growth inhibition when cultures were treated for only 6 or 12 h is interesting (Figure 2A), given that the MEP pathway is known to be active through the entire asexual intraerythrocytic cycle.[18, 23] Analysis of MEP pathway intermediates at ring (12 h post-invasion, hpi), trophozoite (19 hpi) and schizont (33 h post-invasion) showed that IPP concentrations increase markedly between 19 and 33 hpi (Figure 3), which is in agreement with our cytocidal analysis showing that the measured LC_{50} value in cultures exposed for only 24 h was very close to the IC_{50} value measured at 72 h. Cassera and co-workers have previously shown that transcript abundance of genes involved in the MEP pathway, and the isoprenoid products dolichol and ubiquinone all peak at the schizont stage.[23] Therefore, one potential explanation for the lack of growth inhibition observed at 72 h when **1a** was present for only 6 or 12 h is that isoprenoid products were present at a sufficient level at the time that **1a** treatment started to allow parasites to progress through ring and early trophozoite stages until **1a** was washed out.

Methylamide derivative 7a inhibits CDP-ME formation *in vivo* better than the carboxylic acid 1a. In 2015, we reported that the methylamide derivative **7a** was equipotent to **1a** for *P. falciparum* growth inhibition,[13] and in this study, we determined that their *Pf*IspD inhibition values are identical within experimental error (44 ± 15 nM and 57 ± 10 nM respectively, Table 1 and 3). As a further means to compare these compounds, we assessed *in vivo* IspD inhibition in *P. falciparum* at schizont stage by quantitative liquid chromatography-mass spectrometry (LC-MS/MS, Figure 4) in highly synchronous schizont stage parasites treated for 2 and 4 h with 1 μM **1a** or **7a** (~4 times the IC_{50} value). FOS was used as positive control at 10 μM (~10 times the IC_{50} value). After 2 h of drug exposure, **7a** caused 93 ± 5% decrease in the cellular levels of the *Pf*IspD product CDP-ME, while **1a** caused 67 ± 2% decrease. The 27% greater reduction

caused by **7a** was statistically significant by the Benjamini-Hochberg significance test. After 4 h of treatments, **1a** caused 84 ± 8% decrease in the levels of CDP-ME while the reduction caused by **7a** remained the same. Interestingly, FOS treatment did not cause significant reduction of the CDP-ME levels after 2 h nor 4 h of drug exposure. As mentioned above, FOS does not inhibit the enzymatic activity of recombinant *Pf*IspD (Table 1). Previously, Zhang and colleagues reported that parasites treated with 5 μM FOS for 10 h starting at ring stage presented increased levels of MEP and an unknown metabolite, presumptively identified as 2-*C*-methylerythrose 4-phosphate, and reduced levels of CDP-ME.[24] Accumulation of MEP and the potential 2-*C*-methylerythrose 4-phosphate was unexpected and the authors hypothesized that FOS may be indirectly inhibiting *Pf*IspD through the intermediate 2-*C*-methylerythrose 4-phosphate that accumulates following FOS treatment or through other control mechanisms that remain to be identified. Because our experiments involved shorter treatments at a different *P. falciparum* stage, the results cannot be directly compared; however, in both cases FOS induced unexpected levels of metabolites downstream of its enzyme target DXR, suggesting that FOS is triggering other control mechanisms that regulate the MEP pathway in the malaria parasite.

On the other hand, the reduction of the cellular levels of the methylerythritol cyclodiphosphate (MEcPP) and the final MEP pathway product, IPP, did not show significant differences among the three treatments after 2 h and 4 h of exposure to **1a**, **7a** and FOS as assessed by the Benjamini-Hochberg significance test. However, the overall reduction of the MEcPP and IPP levels was greater after 4 h of treatment with the three inhibitors where >90% reduction of the IPP levels was achieved (Figure 4). Overall, these results are in agreement with the results described above showing that **1a** is cytocidal in late trophozoite-early schizont stages where there is a higher demand of isoprenoid products such as dolichol and ubiquinone.[23]

Human IspD is not targeted by 1a. Isoprenoid synthase domain-containing (IspD-like) proteins belong to a large family of glycosyltransferases conserved from bacteria to mammals and

defective function of a IspD-like protein disrupts glycosylation of α-dystroglycan causing Walker–Warburg syndrome, a congenital muscular dystrophy accompanied by a variety of brain and eye malformations.[25-26] Recently, functional studies revealed that human IspD is a ribitol-5-phosphate cytidyltransferase.[27-29] Because of the possibility that drugs directed against IspD enzymes from pathogenic bacteria and parasites could also inhibit the human IspD enzyme causing undesired side effects, the validity of IspD as drug target has been questioned.[29-30] In order to assess if **1a** inhibits human IspD activity, its enzymatic activity was measured by LC-MS/MS to monitor CDP-ribitol formation in the presence of 20 and 200 μM of **1a**. The CDP-ribitol formation was not inhibited by the presence of **1a** at either concentration (Figure 5). This result was expected since **1a** has been shown to be active against *P. falciparum* and *P. vivax* but not bacterial or plant IspD homologues.[12, 14] Therefore, our results support the validity of *Pf*IspD as drug target and the further development of this chemotype for malaria prophylaxis and pharmacotherapy. As other *Pf*IspD inhibitor chemotypes emerge, testing against hIspD will help elucidate the structural basis of this important selectivity.

METHODS

Synthesis of Analogs of 1a. Compound **1a** and its D-ring variants **1b**-**ae** were prepared by Pictet-Spengler reaction of the requisite aldehydes with (*S*)-Trp-OMe as described in Scheme 1. The *trans*-configured methyl ester intermediates **3a**-**ac** were separated from their *cis*-isomers by column chromatography on silica gel (using dichloromethane-ethyl acetate-hexanes mixtures to elute, as described in the Supporting Information). The relative configuration of each isomer was determined by ^{13}C NMR according to Cook's method,[31] and in every case examined thus far, the *cis*-isomer eluted before the *trans*-isomer. Compounds **1h**-**s**, **1w**, **1y**-**af** have not been previously described. C1-Methyl analogs **1ae** and **1af** were prepared by ketone Pictet-Spengler reaction[32] with (*S*)-Trp-OMe (Scheme 2). Note that application of this protocol to 2,4-dichlorophenyl methyl ketone did not give the expected C1-methyl analog of **1a**. Methyl ester

3a, 1° amide **6a**, methyl amides **7a**, **7e**, and (±)-**11a** were prepared as described previously.[13] New methyl amides **7i-k** were prepared by treating the corresponding methyl esters **3i**-**k** with methylamine in ethanol. Ethyl amide **8a** and *N*,*N*-dimethyl amide **9a** were prepared by HATU coupling of **1a** with ethylamine and dimethylamine, respectively. The 1° alcohol analog **10a** was prepared by $LiAlH_4$ reduction of **1a.**

***P. falciparum* Culture.** Parasites Dd2 (MRA-150) strain were maintained in O^+ human erythrocytes at 4% hematocrit in RPMI 1640 media supplemented with 2 g/L glucose (Sigma-Aldrich), 2.3 g/L sodium bicarbonate (Sigma-Aldrich), 50 mg/L hypoxanthine (Sigma-Aldrich), 5.94 g/L HEPES, 20 mg/L gentamycin (GIBCO Life Technologies), and 5 g/L Albumax I (GIBCO Life Technologies). Parasites were kept at 37 ^oC under reduced oxygen conditions (5% CO_2, 5% O_2, and 90% N_2). Synchronous cultures in ring stage (>95%) were obtained by two cycles of 5% sorbitol treatment.

***P. falciparum* Growth Inhibition (IC_{50}) and IPP Reversal of Growth Assays.** The effects of **1a** and analogs were evaluated against *P. falciparum,* Dd2 strain, by SYBR Green assay as described previously in a 72 h assay since we previously reported that this class of apicoplast-targeting compounds do not present a delayed death phenotype.[11] Studies were performed with Dd2 strain since it is chloroquine resistant and we have previously showed that there is no significant differences between resistant and sensitive *P. falciparum* strains.[11] Briefly, ring stage parasite cultures (100 μL per well, with 1% hematocrit and 1% parasitemia) were grown for 72 h in the presence of increasing concentrations of the inhibitor under reduced oxygen conditions (5% CO_2, 5% O_2, and 90% N_2) at 37 ^oC. After 72 h in culture, parasite viability was determined by DNA quantitation using SYBR Green I as described previously.[33] The half-maximum inhibitory concentration (IC_{50}) values were calculated with GraphPad Prism (GraphPad Software, Inc.) using nonlinear regression curve fitting. The reported values represent averages

of at least three independent experiments performed in triplicate, using 10-point serial dilutions, with standard errors of the mean (S.E.M.). The range for serial dilutions was adjusted accordingly for each analog after the first screening to set the IC_{50} value in the middle of the concentration range.

To establish reversal of growth inhibition by IPP, ring stage parasite cultures were grown for 72 h in the presence of increasing concentrations of drug, and in the presence or absence of 200 μM IPP. The reported values represent averages of at least two independent experiments. S.E.M. values are only indicated for mean values below 100%. The parasite's growth inhibition and recovery was assessed by SYBR Green as described previously.[11]

Cytocidal (LC_{50}) Assay. In order to determine the concentration of a bolus dose of the re-synthesized 1*R*,3*S*-MMV008138 (**1a**) that kills 50% of parasites (LC_{50}), *P. falciparum* (Dd2 strain) cultures were exposed to increasing concentrations of **1a** and then the drug was washed away at 6, 12, 18, and 24 h to also probe stage specificity for the activity of **1a** as described previously.[34] Briefly, following the bolus dose incubation, plates were centrifuged at 700 *x* g for 3 min and **1a**-containing medium was removed. Cell pellets were washed three times with 100 μl of medium using the same centrifuge settings and then re-suspended in 100 μl of media without the inhibitor. Washed plates were then incubated at 37 ^{o}C to complete a total of 72 h after setting the assays, and growth of surviving parasites was assessed by SYBR Green. The half-maximum lethal concentration (LC_{50}) values were calculated with GraphPad Prism software (GraphPad Software, Inc.) using nonlinear regression curve fitting, and the reported values represent averages and S.E.M. of at least three independent assays, with each assay performed in triplicate. Parasites untreated or treated with **1a** were smeared and stained with Giemsa before washing the inhibitor in order to assess stage development at the time that **1a** was removed.

***E. coli* Growth Inhibition Assays.** In order to investigate the effect of selected compounds against *E. coli*, strain BL21(DE3), an overnight culture of *E. coli* cultivated at 37 ^{o}C at 200 rpm agitation was diluted 100-fold into LB broth medium and incubated to an OD_{600} of ~0.6. The culture was then diluted 10,000-fold into LB broth medium. Then, 750 µL of this *E. coli* inoculum was inoculated into a culture tube containing 750 µL of the test compounds previously diluted in LB broth medium at three final concentrations (500 µM, 250 µM, and 125 µM). The final DMSO concentration was 5%. Cultures were incubated for 18 h at 37 ^{o}C and 200 rpm agitation. The following controls were performed: 100 µM fosmidomycin (FOS) treatment which targets the MEP pathway in *E. coli*, media without inoculum, 5% DMSO (vehicle), and control with inoculum alone (untreated). After 18h incubation, bacteria growth was measured using a cell density meter. The percentage of growth was normalized to that of untreated control bacteria and potential inhibition of growth of **1a** analogs was determined by comparison to the 5% DMSO control, which does not affect *E. coli* growth, as we described previously.[13] The data represents the mean and S.E.M. of two independent experiments.

***P. falciparum* IspD Protein Purification and IspD enzymatic Assay Conditions.** Plasmid containing wild-type *Pf*IspD (pBG1869 *Pf*IspD) as described in Imlay et al, was a gift from Dr. Audrey Odom.[14] pBG1869 PfIspD was transformed into Arctic Express (DE3) RIL *E. coli* cells (Stratagene), followed by protein expression and purification as described previously (see Supporting Information, Figure S1).[14] The effect of **1a** analogs on inhibiting *Pf*IspD enzymatic activity was measured using PhosphoWorks™ Fluorimetric Pyrophosphate Assay Kit (AAT Bioquest®, Inc.) following manufacturer's instructions.[35-37] This fluorimetric assay directly measures pyrophosphate (PP_i) with a linear range of 0.3 to 30 µM (detection limit of 0.1 µM) as described by the manufacturer. We measured PPi released in the enzymatic reaction catalyzed by *Pf*IspD (MEP + CTP → CDP-ME + PP_i). The reactions were performed in a solid black 96-

well microplate in a final volume of 50 µL (25 µL test samples and 25 µL assay solution) according to the manufacturer's protocol. Briefly, various concentrations of **1a** analogs were incubated for 10 minutes with 60 µM CTP, 60 µM MEP, 100 mM Tris-HCl (pH 7.4) and 1.6 mM $MgCl_2$. Reactions were initiated by adding 60 nM *Pf*IspD. In assays with variable MEP, 100 µM CTP was used and in assays with variable CTP, 100 µM MEP was used. Fluorescence signal was continuously monitored at 316 nm (Ex) and 456 nm (Em) using a Cytation-5 multi-mode plate reader (BioTek). The half-maximum inhibitory concentration (IC_{50}) values were calculated using GraphPad Prism software (GraphPad Software, Inc.) from a 7-data points curve from at least three independent experimental replicates. The data represents the mean and S.E.M. A reaction mix without *Pf*IspD was performed in all assays and used for background subtraction. The range for serial dilutions was adjusted accordingly for each analog after the first screening to set the IC_{50} value in the middle of the concentration range.

Human IspD Protein Enzymatic Assay. Human IspD (hIspD) recombinant protein and its substrate ribitol-5-phosphate were a generous gift from Dr. Lance Wells and Dr. Osman Sheikh (University of Georgia).[28-29] The effect of **1a** on inhibiting hIspD enzymatic activity was measured by LC-MS/MS to monitor CDP-ribitol formation as described below for the detection of the MEP intermediates.[10] Briefly, the enzymatic assay was performed using 2 µM hIspD, 50 mM Tris-HCl (pH 7.2), 2 mM $MgCl_2$, 2 mM DTT, 1 mM CTP and 1 mM ribitol-5-phosphate in the absence or presence of **1a** at 20 and 200 µM. Reactions were carried out at 37 ºC for 16 h. The reported mean and S.E.M values were calculated from two independent assays.

MEP Pathway Metabolite Profiling. Mycoplasma-free parasite cultures were tightly synchronized and grown to recover ring, trophozoite and schizont stages for MEP pathway intermediates level assessment or early schizont stage (~27 h post-invasion) for drug

treatments and MEP pathway intermediates level assessment. Cultures in early schizont stage were treated for 2 and 4 h with 0.1% DMSO (control), 1 μM **1a**, 1 μM **7a** or 10 μM FOS. In all cases, parasites from infected erythrocytes were released from the host cell by lysis with 0.03% saponin in cold PBS containing 2 g/L glucose and washed three times with PBS/glucose by centrifuging 7 min at 10,000 × *g* at 4 °C. Metabolite extraction was performed by adding 250 µL per sample of ice-cold extraction solvent consisting of chloroform, methanol, acetonitrile (2:1:1, v/v/v) containing 1 µM isopentenyl *S*-thiolodiphosphate (ISPP) as internal standard. Samples were sonicated for 10 min in a water bath sonicator with ice. Then, 500 µL of ice-cold MS water was added, mixed by vortex and centrifuged at 12,000 x *g* at 4 °C for 4 min. The polar upper phase was transferred to a 10 kDa centricom tube and centrifuged at 12,000 x *g* at 4 °C for 10 min. The flow through was lyophilized, resuspend in 120 µL of ice-cold MS water and centrifuged at 12,000 *x g* at 4 °C for 10 min. Samples were transferred to a total recovery vial (Waters) and two injections of 40 µL of each sample underwent LC-MS/MS analysis as previously described using ion-pair reversed phase ultra-performance liquid chromatography in tandem with mass spectrometry (IP-RP-UPLC-MS/MS).[38] Data were acquired using MassLynx Software, v. 4.1, and processed using TargetLynx™ Application Manager (Waters). Relative quantification of the level of each metabolite was performed by determining the analyte-to-internal standard ratio (response) calculated by dividing the area of the analyte peak by the area of the internal standard (ISPP) peak. The response of each detected metabolite is expressed as the mean and S.E.M. of two biological replicates.

ACKNOWLEDGMENTS

We thank the National Institutes of Health (AI128362 (PRC), AI082581 (PRC), and AI108819 (MBC)), the Fralin Life Science Institute at Virginia Tech, and the Virginia Tech Center for Drug Discovery, for financial support. The following reagent was obtained through the MR4 as part of the BEI Resources Repository, NIAID, NIH: *Plasmodium falciparum* Dd2 strain, MRA-150,

deposited by D Walliker. We thank Dr. Audrey Odom (Washington University) for the gift of the plasmid containing *Pf*IspD for protein expression. We thank Dr. Lance Wells and Dr. M. Osman Sheikh for the gift if the human IspD protein and ribitol-5-phosphate.

ASSOCIATED CONTENT

Supporting Information

The following file (45 pages) is available free of charge on the ACS Publications website doi:xxxx. Synthetic procedures and analytical characterization data for all the new compounds described in the paper, SDS-PAGE analysis of the *Pf*IspD used for enzyme inhibition studies (Figure S1), and determination of kinetic parameters for *Pf*IspD (Figure S2).

Abbreviations

MEP, methylerythritol phosphate; IPP, isopentenyl pyrophosphate; DMAPP, dimethylallyl pyrophosphate; CTP, cytidine diphosphate; CDP-ME, cytidine diphosphate methylerythritol; MEcPP, methylerythritol cyclodiphosphate; FOS, fosmidomycin; SAR, structure-activity relationships; hpi, hours post-invasion; IC_{50}, half-maximum inhibitory concentration; LC_{50}, half-maximum lethal concentration.

Author Contributions

The study and experiments were designed by M.B.C, P.R.C., D.J.S., M.M.T., M.G., E.F.M., Z-K.Y., R.E., M.E.S., M.L.F-M., J.H.B., M.A.C., P.M.K. Experiments were conducted by M.G., E.F.M., Z-K.Y., R.E., M.E.S., M.L.F-M., J.H.B., M.A.C., P.M.K. All authors analyzed the data. M.B.C., P.R.C., M.G., M.M.T., and D.J.S. wrote the manuscript, and all authors have read and given approval to the final version.

REFERENCES

1. WHO, World Malaria Report 2015, World Health Organization **2016**.
2. Spangenberg, T.; Burrows, J. N.; Kowalczyk, P.; McDonald, S.; Wells, T. N. C.; Willis, P., The Open Access Malaria Box: A Drug Discovery Catalyst for Neglected Diseases. *PLOS One* **2013,** *8* (6), e62906. DOI: 10.1371/journal.pone.0062906.
3. Guiguemde, W. A.; Shelat, A. A.; Garcia-Bustos, J. F.; Diagana, T. T.; Gamo, F. J.; Guy, R. K., Global phenotypic screening for antimalarials. *Chem Biol* **2012,** *19* (1), 116-29. DOI: 10.1016/j.chembiol.2012.01.004.
4. Van Voorhis, W. C.; Adams, J. H.; Adelfio, R.; Ahyong, V.; Akabas, M. H.; Alano, P.; Alday, A.; Aleman Resto, Y.; Alsibaee, A.; Alzualde, A.; Andrews, K. T.; Avery, S. V.; Avery, V. M.; Ayong, L.; Baker, M.; Baker, S.; Ben Mamoun, C.; Bhatia, S.; Bickle, Q.; Bounaadja, L.; Bowling, T.; Bosch, J.; Boucher, L. E.; Boyom, F. F.; Brea, J.; Brennan, M.; Burton, A.; Caffrey, C. R.; Camarda, G.; Carrasquilla, M.; Carter, D.; Belen Cassera, M.; Chih-Chien Cheng, K.; Chindaudomsate, W.; Chubb, A.; Colon, B. L.; Colon-Lopez, D. D.; Corbett, Y.; Crowther, G. J.; Cowan, N.; D'Alessandro, S.; Le Dang, N.; Delves, M.; DeRisi, J. L.; Du, A. Y.; Duffy, S.; Abd El-Salam El-Sayed, S.; Ferdig, M. T.; Fernandez Robledo, J. A.; Fidock, D. A.; Florent, I.; Fokou, P. V.; Galstian, A.; Gamo, F. J.; Gokool, S.; Gold, B.; Golub, T.; Goldgof, G. M.; Guha, R.; Guiguemde, W. A.; Gural, N.; Guy, R. K.; Hansen, M. A.; Hanson, K. K.; Hemphill, A.; Hooft van Huijsduijnen, R.; Horii, T.; Horrocks, P.; Hughes, T. B.; Huston, C.; Igarashi, I.; Ingram-Sieber, K.; Itoe, M. A.; Jadhav, A.; Naranuntarat Jensen, A.; Jensen, L. T.; Jiang, R. H.; Kaiser, A.; Keiser, J.; Ketas, T.; Kicka, S.; Kim, S.; Kirk, K.; Kumar, V. P.; Kyle, D. E.; Lafuente, M. J.; Landfear, S.; Lee, N.; Lee, S.; Lehane, A. M.; Li, F.; Little, D.; Liu, L.; Llinas, M.; Loza, M. I.; Lubar, A.; Lucantoni, L.; Lucet, I.; Maes, L.; Mancama, D.; Mansour, N. R.; March, S.; McGowan, S.; Medina Vera, I.; Meister, S.; Mercer, L.; Mestres, J.; Mfopa, A. N.; Misra, R. N.; Moon, S.; Moore, J. P.; Morais Rodrigues da Costa, F.; Muller, J.; Muriana, A.; Nakazawa Hewitt, S.; Nare, B.; Nathan, C.; Narraidoo, N.; Nawaratna, S.; Ojo, K. K.; Ortiz, D.; Panic, G.; Papadatos, G.; Parapini, S.; Patra, K.; Pham, N.; Prats, S.; Plouffe, D. M.; Poulsen, S. A.; Pradhan, A.; Quevedo, C.; Quinn, R. J.; Rice, C. A.; Abdo Rizk, M.; Ruecker, A.; St Onge, R.; Salgado Ferreira, R.; Samra, J.; Robinett, N. G.; Schlecht, U.; Schmitt, M.; Silva Villela, F.; Silvestrini, F.; Sinden, R.; Smith, D. A.; Soldati, T.; Spitzmuller, A.; Stamm, S. M.; Sullivan, D. J.; Sullivan, W.; Suresh, S.; Suzuki, B. M.; Suzuki, Y.; Swamidass, S. J.; Taramelli, D.; Tchokouaha, L. R.; Theron, A.; Thomas, D.; Tonissen, K. F.; Townson, S.; Tripathi, A. K.; Trofimov, V.; Udenze, K. O.; Ullah, I.; Vallieres, C.; Vigil, E.; Vinetz, J. M.; Voong Vinh, P.; Vu, H.; Watanabe, N. A.; Weatherby, K.; White, P. M.; Wilks, A. F.; Winzeler, E. A.; Wojcik, E.; Wree, M.; Wu, W.; Yokoyama, N.; Zollo, P. H.; Abla, N.; Blasco, B.; Burrows, J.; Laleu, B.; Leroy, D.; Spangenberg, T.; Wells, T.; Willis, P. A., Open Source Drug Discovery with the Malaria Box Compound Collection for Neglected Diseases and Beyond. *PLoS Pathog* **2016,** *12* (7), e1005763. DOI: 10.1371/journal.ppat.1005763.
5. Goodman, C. D.; McFadden, G. I., Targeting apicoplasts in malaria parasites. *Expert Opin Ther Targets* **2013,** *17* (2), 167-77. DOI: 10.1517/14728222.2013.739158.
6. van Dooren, G. G.; Striepen, B., The algal past and parasite present of the apicoplast. *Annu Rev Microbiol* **2013,** *67*, 271-89. DOI: 10.1146/annurev-micro-092412-155741.
7. Odom, A. R.; Van Voorhis, W. C., Functional genetic analysis of the Plasmodium falciparum deoxyxylulose 5-phosphate reductoisomerase gene. *Mol Biochem Parasitol* **2010,** *170* (2), 108-11. DOI: 10.1016/j.molbiopara.2009.12.001.
8. Nair, S. C.; Brooks, C. F.; Goodman, C. D.; Sturm, A.; McFadden, G. I.; Sundriyal, S.; Anglin, J. L.; Song, Y.; Moreno, S. N.; Striepen, B., Apicoplast isoprenoid precursor synthesis and the molecular basis of fosmidomycin resistance in Toxoplasma gondii. *J Exp Med* **2011,** *208* (7), 1547-59. DOI: 10.1084/jem.20110039.

9. Yeh, E.; DeRisi, J. L., Chemical rescue of malaria parasites lacking an apicoplast defines organelle function in blood-stage Plasmodium falciparum. *PLoS Biol* **2011,** *9* (8), e1001138. DOI: 10.1371/journal.pbio.1001138.
10. Wiley, J. D.; Merino, E. F.; Krai, P. M.; McLean, K. J.; Tripathi, A. K.; Vega-Rodriguez, J.; Jacobs-Lorena, M.; Klemba, M.; Cassera, M. B., Isoprenoid precursor biosynthesis is the essential metabolic role of the apicoplast during gametocytogenesis in Plasmodium falciparum. *Eukaryot Cell* **2015,** *14* (2), 128-39. DOI: 10.1128/EC.00198-14.
11. Bowman, J. D.; Merino, E. F.; Brooks, C. F.; Striepen, B.; Carlier, P. R.; Cassera, M. B., Antiapicoplast and gametocytocidal screening to identify the mechanisms of action of compounds within the malaria box. *Antimicrob Agents Chemother* **2014,** *58* (2), 811-9. DOI: 10.1128/AAC.01500-13.
12. Wu, W.; Herrera, Z.; Ebert, D.; Baska, K.; Cho, S. H.; DeRisi, J. L.; Yeh, E., A chemical rescue screen identifies a Plasmodium falciparum apicoplast inhibitor targeting MEP isoprenoid precursor biosynthesis. *Antimicrob Agents Chemother* **2015,** *59* (1), 356-64. DOI: 10.1128/AAC.03342-14.
13. Yao, Z. K.; Krai, P. M.; Merino, E. F.; Simpson, M. E.; Slebodnick, C.; Cassera, M. B.; Carlier, P. R., Determination of the active stereoisomer of the MEP pathway-targeting antimalarial agent MMV008138, and initial structure-activity studies. *Bioorg Med Chem Lett* **2015,** *25* (7), 1515-9. DOI: 10.1016/j.bmcl.2015.02.020.
14. Imlay, L. S.; Armstrong, C. M.; Masters, M. C.; Li, T.; Price, K. E.; Edwards, R. L.; Mann, K. M.; Li, L. X.; Stallings, C. L.; Berry, N. G.; O'Neill, P. M.; Odom, A. R., Plasmodium IspD (2-C-Methyl-D-erythritol 4-Phosphate Cytidyltransferase), an Essential and Druggable Antimalarial Target. *ACS Infect Dis* **2015,** *1* (4), 157-167. DOI: 10.1021/id500047s.
15. Gill, S. R.; Pop, M.; Deboy, R. T.; Eckburg, P. B.; Turnbaugh, P. J.; Samuel, B. S.; Gordon, J. I.; Relman, D. A.; Fraser-Liggett, C. M.; Nelson, K. E., Metagenomic analysis of the human distal gut microbiome. *Science* **2006,** *312* (5778), 1355-9. DOI: 10.1126/science.1124234.
16. Dahl, E. L.; Shock, J. L.; Shenai, B. R.; Gut, J.; DeRisi, J. L.; Rosenthal, P. J., Tetracyclines specifically target the apicoplast of the malaria parasite Plasmodium falciparum. *Antimicrob Agents Chemother* **2006,** *50* (9), 3124-31. DOI: 10.1128/AAC.00394-06.
17. Dahl, E. L.; Rosenthal, P. J., Apicoplast translation, transcription and genome replication: targets for antimalarial antibiotics. *Trends Parasitol* **2008,** *24* (6), 279-84. DOI: 10.1016/j.pt.2008.03.007.
18. Cassera, M. B.; Gozzo, F. C.; D'Alexandri, F. L.; Merino, E. F.; del Portillo, H. A.; Peres, V. J.; Almeida, I. C.; Eberlin, M. N.; Wunderlich, G.; Wiesner, J.; Jomaa, H.; Kimura, E. A.; Katzin, A. M., The methylerythritol phosphate pathway is functionally active in all intraerythrocytic stages of Plasmodium falciparum. *J Biol Chem* **2004,** *279* (50), 51749-59. DOI: 10.1074/jbc.M408360200.
19. Jomaa, H.; Wiesner, J.; Sanderbrand, S.; Altincicek, B.; Weidemeyer, C.; Hintz, M.; Turbachova, I.; Eberl, M.; Zeidler, J.; Lichtenthaler, H. K.; Soldati, D.; Beck, E., Inhibitors of the nonmevalonate pathway of isoprenoid biosynthesis as antimalarial drugs. *Science* **1999,** *285* (5433), 1573-6.
20. Tan, K. R.; Magill, A. J.; Parise, M. E.; Arguin, P. M.; Centers for Disease, C.; Prevention, Doxycycline for malaria chemoprophylaxis and treatment: report from the CDC expert meeting on malaria chemoprophylaxis. *Am J Trop Med Hyg* **2011,** *84* (4), 517-31. DOI: 10.4269/ajtmh.2011.10-0285.
21. Scholfield, M. R.; Zanden, C. M. V.; Carter, M.; Ho, P. S., Halogen bonding (X-bonding): A biological perspective. *Protein. Sci.* **2013,** *22* (2), 139-152. DOI: 10.1002/pro.2201.
22. Kunfermann, A.; Witschel, M.; Illarionov, B.; Martin, R.; Rottmann, M.; Höffken, H. W.; Seet, M.; Eisenreich, W.; Knölker, H.-J.; Fischer, M.; Bacher, A.; Groll, M.; Diederich, F.,

Pseudilins: Halogenated, Allosteric Inhibitors of the Non-Mevalonate Pathway Enzyme IspD. *Angew. Chem. Int. Ed.* **2014,** *53* (8), 2235-2239. DOI: 10.1002/anie.201309557.
23. Cassera, M. B.; Merino, E. F.; Peres, V. J.; Kimura, E. A.; Wunderlich, G.; Katzin, A. M., Effect of fosmidomycin on metabolic and transcript profiles of the methylerythritol phosphate pathway in Plasmodium falciparum. *Mem Inst Oswaldo Cruz* **2007,** *102* (3), 377-83.
24. Zhang, B.; Watts, K. M.; Hodge, D.; Kemp, L. M.; Hunstad, D. A.; Hicks, L. M.; Odom, A. R., A second target of the antimalarial and antibacterial agent fosmidomycin revealed by cellular metabolic profiling. *Biochemistry* **2011,** *50* (17), 3570-7. DOI: 10.1021/bi200113y.
25. Roscioli, T.; Kamsteeg, E. J.; Buysse, K.; Maystadt, I.; van Reeuwijk, J.; van den Elzen, C.; van Beusekom, E.; Riemersma, M.; Pfundt, R.; Vissers, L. E.; Schraders, M.; Altunoglu, U.; Buckley, M. F.; Brunner, H. G.; Grisart, B.; Zhou, H.; Veltman, J. A.; Gilissen, C.; Mancini, G. M.; Delree, P.; Willemsen, M. A.; Ramadza, D. P.; Chitayat, D.; Bennett, C.; Sheridan, E.; Peeters, E. A.; Tan-Sindhunata, G. M.; de Die-Smulders, C. E.; Devriendt, K.; Kayserili, H.; El-Hashash, O. A.; Stemple, D. L.; Lefeber, D. J.; Lin, Y. Y.; van Bokhoven, H., Mutations in ISPD cause Walker-Warburg syndrome and defective glycosylation of alpha-dystroglycan. *Nat Genet* **2012,** *44* (5), 581-5. DOI: 10.1038/ng.2253.
26. Willer, T.; Lee, H.; Lommel, M.; Yoshida-Moriguchi, T.; de Bernabe, D. B.; Venzke, D.; Cirak, S.; Schachter, H.; Vajsar, J.; Voit, T.; Muntoni, F.; Loder, A. S.; Dobyns, W. B.; Winder, T. L.; Strahl, S.; Mathews, K. D.; Nelson, S. F.; Moore, S. A.; Campbell, K. P., ISPD loss-of-function mutations disrupt dystroglycan O-mannosylation and cause Walker-Warburg syndrome. *Nat Genet* **2012,** *44* (5), 575-80. DOI: 10.1038/ng.2252.
27. Gerin, I.; Ury, B.; Breloy, I.; Bouchet-Seraphin, C.; Bolsee, J.; Halbout, M.; Graff, J.; Vertommen, D.; Muccioli, G. G.; Seta, N.; Cuisset, J. M.; Dabaj, I.; Quijano-Roy, S.; Grahn, A.; Van Schaftingen, E.; Bommer, G. T., ISPD produces CDP-ribitol used by FKTN and FKRP to transfer ribitol phosphate onto alpha-dystroglycan. *Nat Commun* **2016,** *7*, 11534. DOI: 10.1038/ncomms11534.
28. Praissman, J. L.; Willer, T.; Sheikh, M. O.; Toi, A.; Chitayat, D.; Lin, Y. Y.; Lee, H.; Stalnaker, S. H.; Wang, S.; Prabhakar, P. K.; Nelson, S. F.; Stemple, D. L.; Moore, S. A.; Moremen, K. W.; Campbell, K. P.; Wells, L., The functional O-mannose glycan on alpha-dystroglycan contains a phospho-ribitol primed for matriglycan addition. *Elife* **2016,** *5*. DOI: 10.7554/eLife.14473.
29. Riemersma, M.; Froese, D. S.; van Tol, W.; Engelke, U. F.; Kopec, J.; van Scherpenzeel, M.; Ashikov, A.; Krojer, T.; von Delft, F.; Tessari, M.; Buczkowska, A.; Swiezewska, E.; Jae, L. T.; Brummelkamp, T. R.; Manya, H.; Endo, T.; van Bokhoven, H.; Yue, W. W.; Lefeber, D. J., Human ISPD Is a Cytidyltransferase Required for Dystroglycan O-Mannosylation. *Chem Biol* **2015,** *22* (12), 1643-52. DOI: 10.1016/j.chembiol.2015.10.014.
30. Perez-Gil, J.; Rodriguez-Concepcion, M., Metabolic plasticity for isoprenoid biosynthesis in bacteria. *Biochem J* **2013,** *452* (1), 19-25. DOI: 10.1042/BJ20121899.
31. Ungemach, F.; Soerens, D.; Weber, R.; DiPierro, M.; Campos, O.; Mokry, P.; Cook, J. M.; Silverton, J. V., General method for the assignment of stereochemistry of 1,3-disubstituted 1,2,3,4-tetrahydro-β-carbolines by carbon-13 spectroscopy. *J. Am. Chem. Soc.* **1980,** *102* (23), 6976-6984. DOI: 10.1021/ja00543a012.
32. Horiguchi, Y.; Nakamura, M.; Saitoh, T.; Sano, T., A Syntheis of Chiral 1,1,3-Trisubstituted 1,2,3,4-Tetrahydro-β-carbolines by the Pictet-Spengler Reaction of Tryptophan and Ketones: Conversion of (1*R*,3*S*)-Diastereomers into their (1*S*,3*S*)-Counterparts by Scission of the C(1)-N(2) bond. *Chem. Pharm. Bull.* **2003,** *51* (12), 1368-1373.
33. Smilkstein, M.; Sriwilaijaroen, N.; Kelly, J. X.; Wilairat, P.; Riscoe, M., Simple and inexpensive fluorescence-based technique for high-throughput antimalarial drug screening. *Antimicrob Agents Chemother* **2004,** *48* (5), 1803-6.

34. Paguio, M. F.; Bogle, K. L.; Roepe, P. D., Plasmodium falciparum resistance to cytocidal versus cytostatic effects of chloroquine. *Mol Biochem Parasitol* **2011,** *178* (1-2), 1-6. DOI: 10.1016/j.molbiopara.2011.03.003.
35. King, D. T.; Wasney, G. A.; Nosella, M.; Fong, A.; Strynadka, N. C., Structural Insights into Inhibition of Escherichia coli Penicillin-binding Protein 1B. *J Biol Chem* **2017,** *292* (3), 979-993. DOI: 10.1074/jbc.M116.718403.
36. Sabra, A.; Bessoule, J. J.; Atanasova-Penichon, V.; Noel, T.; Dementhon, K., Host-pathogen interaction and signaling molecule secretion are modified in the dpp3 knockout mutant of Candida lusitaniae. *Infect Immun* **2014,** *82* (1), 413-22. DOI: 10.1128/IAI.01263-13.
37. Wang, M.; Yang, X.; Ren, L.; Li, S.; He, X.; Wu, X.; Liu, T.; Lin, L.; Li, Y.; Sun, C., Biomarkers identified by urinary metabonomics for noninvasive diagnosis of nutritional rickets. *J Proteome Res* **2014,** *13* (9), 4131-42. DOI: 10.1021/pr500517u.
38. Laourdakis, C. D.; Merino, E. F.; Neilson, A. P.; Cassera, M. B., Comprehensive quantitative analysis of purines and pyrimidines in the human malaria parasite using ion-pairing ultra-performance liquid chromatography-mass spectrometry. *J Chromatogr B Analyt Technol Biomed Life Sci* **2014,** *967*, 127-33. DOI: 10.1016/j.jchromb.2014.07.012.

Figure 1. MMV008138 as originally disclosed, its active stereoisomer **1a** ((1*R*,3*S*)-MMV008138), and selected analogs.

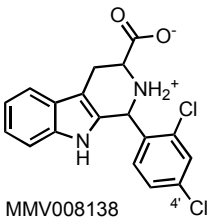

MMV008138

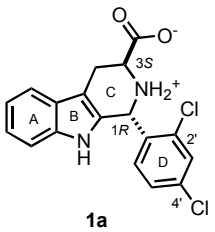

1a
(1*R*,3*S*)-MMV008138

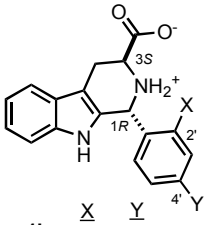

	X	Y
1b	H	H
1c	Cl	H
1e	Cl	Me
1u	Me	Me

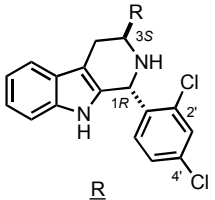

	R
3a	CO_2Me
6a	$CONH_2$
7a	CONHMe
(±)-**11a**	H

Scheme 1. Synthesis of **1a** and its D-ring analogs.

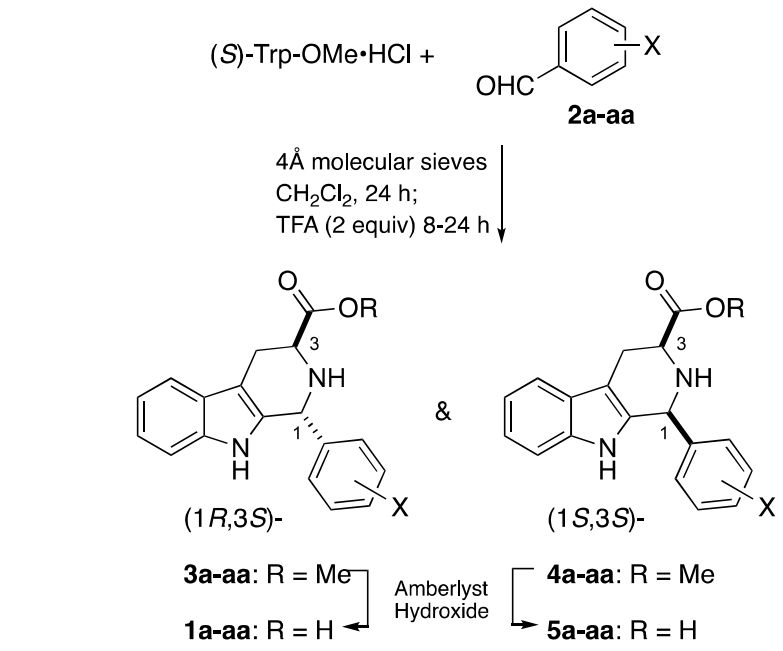

a 2',4'-Cl_2
b H
c 2'-Cl
d 4'-Cl
e 2'-Cl,4'-Me
f 2'-Me,4'-Cl
g 2',4'-F_2
h 2'-F,4'-Cl
i 2'-Cl,4'-F
j 2'-Cl,4'-Br
k 2'-Br,4'-Cl
l 2',4'-Br_2
m 2'-I, 4'-F
n 2'-F,4'-I
o 2'-Br, 4'-I
p 2'-Cl, 4'-OMe
q 2'-OMe, 4'-Cl
r 2'-Cl, 4-OH
s 2'-Cl,4'-CO_2H
t 2',4'-$(CF_3)_2$
u 2',4'-Me_2
v 2',4'-$(OMe)_2$
w 3',4'-Cl_2
x 3',4'-$(OMe)_2$
y 2',6'-F_2,'4-Cl
z 2',3',4'-F_3
aa 2'-Br,4'-F,5'-OMe

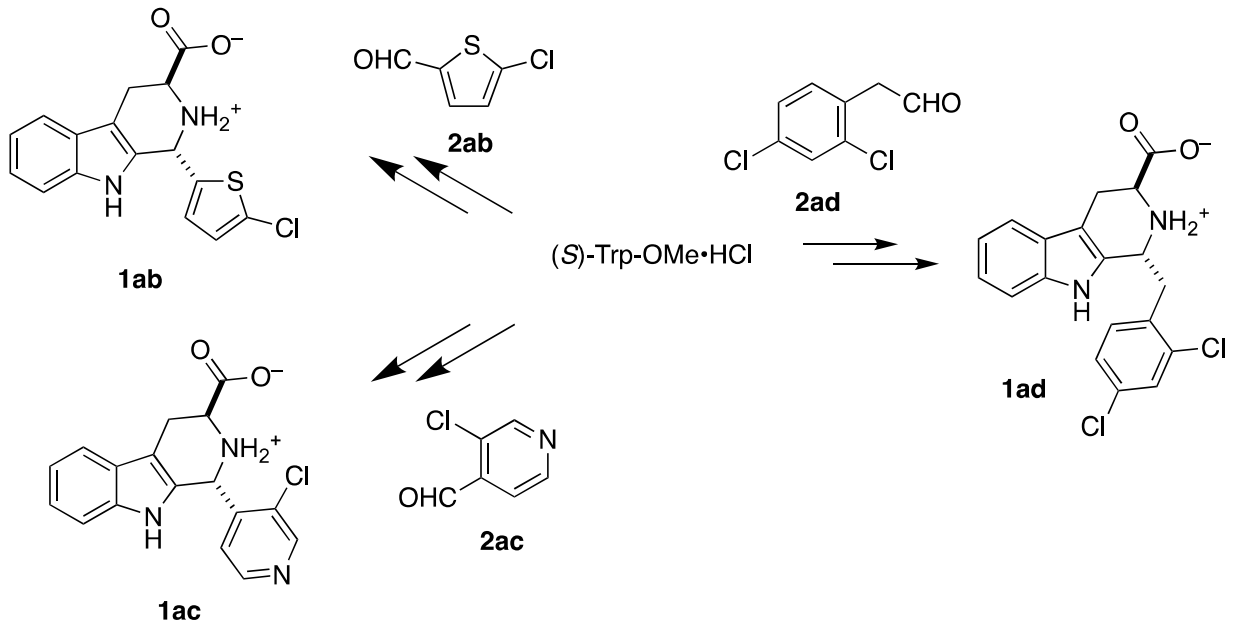

Scheme 2. Synthesis of C1-methyl analogs of **1a**.

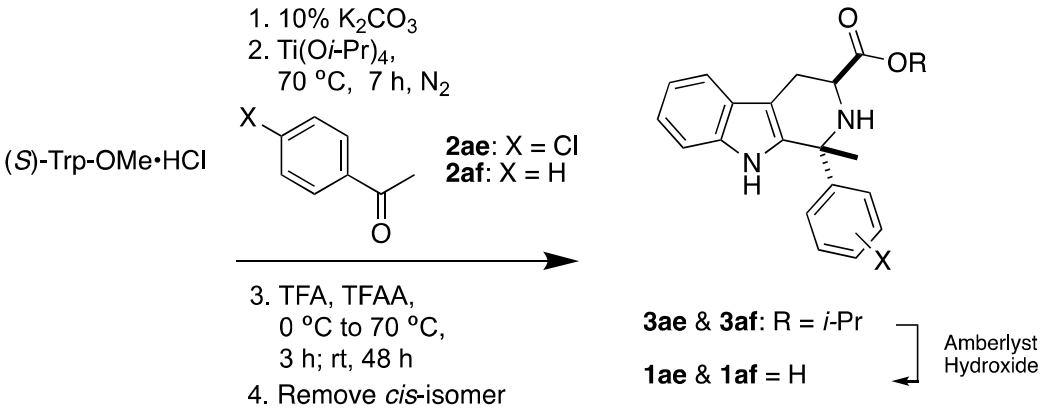

Table 1. *Pf*IspD inhibition potency of MMV008138 stereoisomers and FOS.

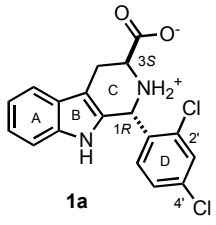

1a

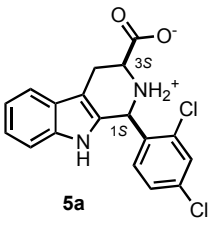

5a

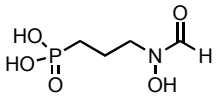

Fosmidomycin (FOS)

Compound	configuration	*P. falciparum* growth inhibition IC_{50} (nM)[a]	% Recovery (200 μM IPP)[c]	*Pf*IspD IC_{50} (nM)[d]	% *E. coli* growth inhibition (18 h)[e]
1a	(1*R*,3*S*)	250 ± 70[b]	100 @ 2.5 μM[b]	44 ± 15	NI @ 500 μM[b]
5a	(1*S*,3*S*)	>10,000[b]	ND[b]	0% inh. @ 1 μM	NI @ 125 μM
ent-**1a**	(1*S*,3*R*)	>10,000[b]	ND[b]	0% inh. @ 1 μM	NI @ 250 μM
ent-**5a**	(1*R*,3*R*)	3,000 ± 200[b]	60 ± 5 @ 10 μM[b]	27 ± 5 % inh. @ 1 μM	18 ± 6 @ 250 μM
FOS	NA	880 ± 70[b]	100[b]	4 ± 2 % inh. @ 10 μM	11.99 ± 0.02 μM (MIC)

[a]MRA-150, chloroquine-resistant (intermediate), pyrimethamine-resistant, mefloquine-resistant. [b]Data reported previously.[13] [c]Drug at indicated concentration; ND signifies 'not determined.' [d]Recombinant *P. falciparum* IspD IC_{50} values measured at [*Pf*IspD] of 60 nM. [e]Percent growth inhibition at the indicated concentration (NI signifies 'no inhibition'), or the minimum inhibitory concentration (MIC). Values represent averages of at least two independent assays ± S.E.M.

Table 2. Growth inhibition (*P. falciparum*, *E. coli*) and *Pf*lspD inhibition of D-ring variants of **1a**.

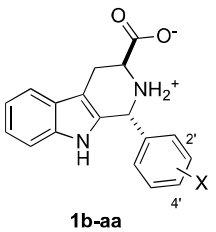

1b-aa

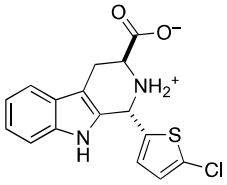

1ab

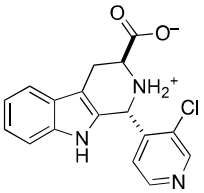

1ac

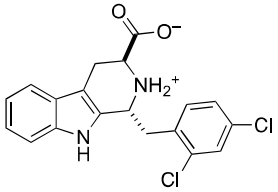

1ad

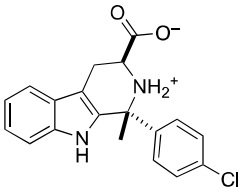

1ae

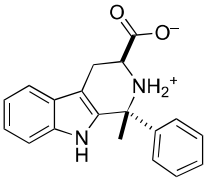

1af

Compound[a]	X	*P. falciparum* growth inhibition IC_{50} (nM)[c]	% Recovery (200 μM IPP)[e]	*Pf*lspD IC_{50} (nM)[f]	*% E. coli* growth inhibition (18 h)[h]
1b	H	>10,000[d]	ND	>5,000[g]	NI @ 250 μM
1c	2'-Cl	3,280 ± 990[d]	60 ± 5 @ 10 μM	~1,000	NI @ 250 μM
1d	4'-Cl	1,170 ± 60[d]	50 ± 7 @ 10 μM	510 ± 90	NI @ 250 μM
1e	2'-Cl,4'-Me	410 ± 40[d]	100 @ 2.5 μM	82 ± 10	NI @ 500 μM[c]
1f	2'-Me, 4'-Cl	700 ± 90[d]	100 @ 2.5 μM	260 ± 50	NI @ 500 μM[c]
1g	2',4'-F_2	780 ± 175[d]	100 @ 5 μM	230 ± 10	NI @ 500 μM[c]
1h	2'-F, 4'-Cl	860 ± 80	100 @ 5 μM	140 ± 30	NI @ 250 μM
1i	2'-Cl,4'-F	433 ± 55	100 @ 10 μM	100 ± 10	NI @ 250 μM
1j	2'-Cl, 4'-Br	320 ± 60	100 @ 5 μM	34 ± 11	NI @ 250 μM
1k	2'-Br,4'-Cl	360 ± 40	100 @ 5 μM	31 ± 4	NI @ 125 μM
1l	2',4'-Br_2	590 ± 20	100 @ 10 μM	84 ± 14	NI @ 125 μM
1m	2'-I, 4'-F	970 ± 180	100 @ 10 μM	140 ± 70	NI @ 250 μM
1n	2'-F, 4'-I	3343 ± 496	100 @ 10 μM	130 ± 20	NI @ 125 μM
1o	2'-Br, 4'-I	1,500 ± 200	80 ± 5 @ 10 μM	ND	ND
1p	2'-Cl, 4'-OMe	>5,000	ND	ND	ND
1q	2'-OMe, 4'-Cl	2,500 ± 600	ND	ND	ND
1r[b]	2'-Cl, 4'-OH	>5,000	ND	ND	ND
1s	2'-Cl, 4'-CO_2H	0% inh. @ 10,000	ND	ND	ND
1t	2',4'-$(CF_3)_2$	>10,000[d]	ND	>5,000[g]	NI @ 250 μM
1u	2',4'-Me_2	70% inh. @ 10,000[d]	ND	~1,000	NI @ 250 μM
1v	2',4'-$(OMe)_2$	>20,000[d]	ND	>5,000[g]	NI @ 250 μM
1w	3',4'-Cl_2	>10,000	ND	0% inh. @ 500 nM	NI @ 250 μM
1x	3',4'-$(OMe)_2$	>20,000[d]	ND	ND	ND
1y	2',6'-F_2,4'-Cl	1,800 ± 150	80 ± 8 @ 10 μM	ND	ND
1z	2',3',4'-F_3	~ 20,000	ND	ND	ND
1aa	2'-Br, 4'-F, 5'-OMe	>10,000	ND	ND	ND
1ab	na	>10,000	ND	ND	ND
1ac	na	> 5,000	ND	ND	ND
1ad	na	>10,000	ND	ND	ND
1ae	na	>10,000	ND	ND	ND
1af	na	>5,000	ND	ND	ND

[a]All compounds are *trans*-configured and derived from (*S*)-Trp-OMe; all are (1*R*,3*S*) except for **1ac**, which is (1*S*,*3S*) due to a Cahn-Ingold-Prelog priority switch. [b]This compound was tested as an approximate 1:1 mixture of the (1*R*,3*S*) and (1*S*,3*S*)-stereoisomers. [c]MRA-150, chloroquine-resistant (intermediate), pyrimethamine-resistant, mefloquine-resistant. [d]Data reported previously.[13] [e]Drug at indicated concentration; ND signifies 'not determined.' [f]Recombinant *P. falciparum* lspD IC_{50} values measured at [*Pf*lspD] of 60 nM. [g]Approximately 10% inhibition at 1,000 nM. [h]Percent growth inhibition at the indicated concentration; NI signifies 'no inhibition.' Values represent averages of at least two independent assays ± S.E.M.

Table 3. Growth inhibition (*P. falciparum*, *E. coli*) and *Pf*lspD inhibition of C3-carboxy replacement variants of **1a**.

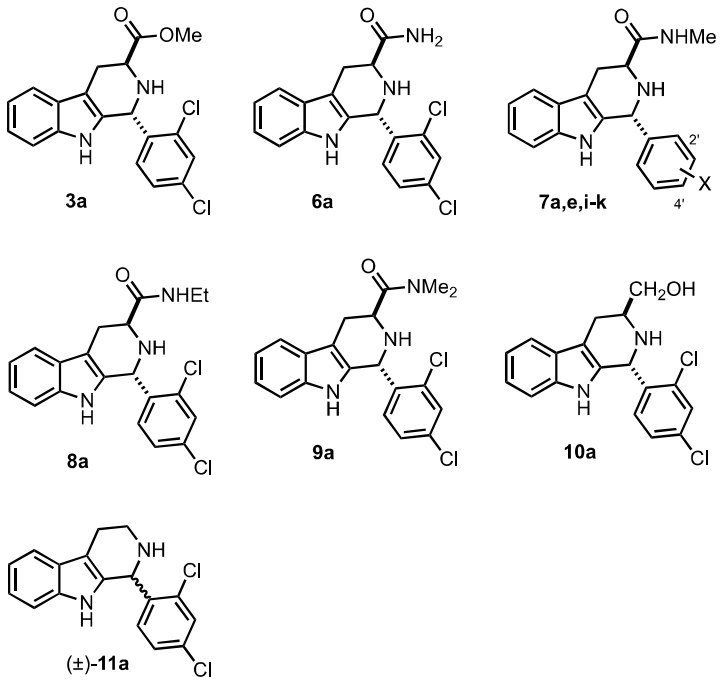

Compound[a]	X	*P. falciparum* growth inhibition IC_{50} (nM)[b]	% Recovery (200 μM IPP)[d]	*Pf*lspD IC_{50} (nM)[e]	% *E. coli* growth inhibition (18 h)[f]
3a	2',4'-Cl_2	6,800 ± 1400[c]	20 ± 10 @ 20 μM	0% inh. @ 1,000	NI @ 250 μM
6a	2',4'-Cl_2	1,200 ± 100[c]	50 ± 7 @ 10 μM	~1,000	NI @ 250 μM
7a	2',4'-Cl_2	190 ± 30[c]	100 @ 2.5 μM	57 ± 10	NI @ 500 μM[c]
7e	2'-Cl, 4'-Me	340 ± 50[c]	100 @ 2.5 μM	360 ± 40	NI @ 500 μM[c]
7i	2'-Cl, 4'-F	506 ± 45	100 @ 2.5 μM	278 ± 27	21 ± 3 @ 250 μM
7j	2'-Cl,4'-Br	300 ± 40	100 @ 5 μM	21 ± 6	NI @ 250 μM
7k	2'-Br, 4'-Cl	340 ± 60	100 @ 5 μM	31 ± 4	NI @ 250 μM
8a	2',4'-Cl_2	~5,000	ND	~1,000	NI @ 250 μM
9a	2',4'-Cl_2	> 20,000	ND	~5% inh. @ 1,000	NI @ 250 μM
10a	2',4'-Cl_2	>10,000	ND	ND	ND
11a	2',4'-Cl_2	10,000 ± 1,600[c]	0 @ 20 μM	7% inh. @ 1,000	45 ± 10 @ 250 μM

[a]All compounds are *trans*-configured, derived from (*S*)-Trp-OMe, and are (1*R*,3*S*). [b]MRA-150, chloroquine-resistant (intermediate), pyrimethamine-resistant, mefloquine-resistant. [c]Data reported previously.[13] [d]Drug at indicated concentration; ND signifies 'not determined.' [e]Recombinant *P. falciparum* lspD IC_{50} values measured at [*Pf*lspD] of 60 nM. [f]Percent growth inhibition at the indicated concentration; NI signifies 'no inhibition.' Values represent averages of at least two independent assays ± S.E.M.

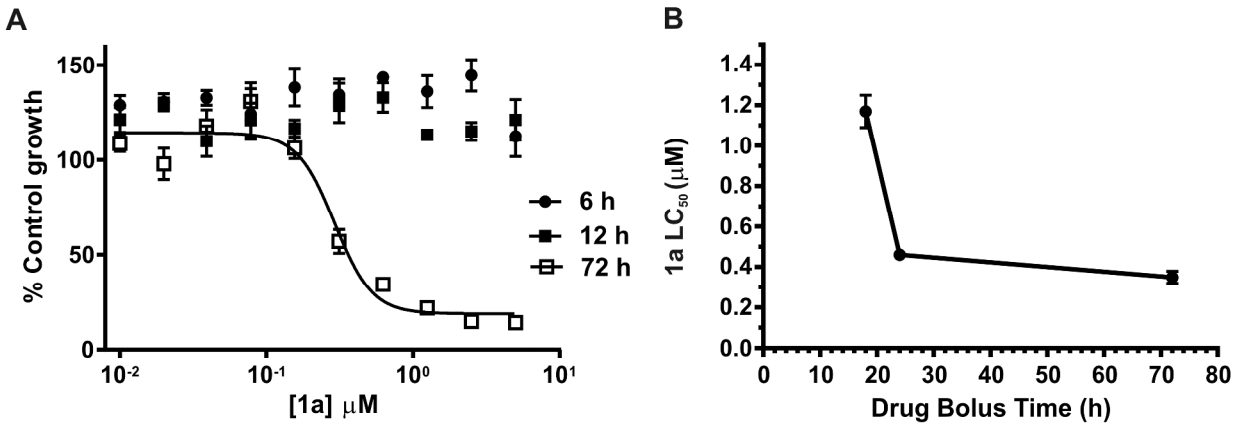

Figure 2. LC_{50} value of **1a** decreases with increasing drug exposure time. (A) Parasite growth was measured at 72 h by SYBR Green assay in cultures where **1a** was washed out at 6 or 12 h, and parasites were returned to culture to complete 72 h. A representative growth inhibition curve at 72 h from parasites continuously exposed to **1a** is also shown. (B) **1a** becomes cytocidal at 18 h drug bolus time when parasites reach late-trophozoite/early schizont stages. The reported values represent averages and S.E.M. of at least three independent assays.

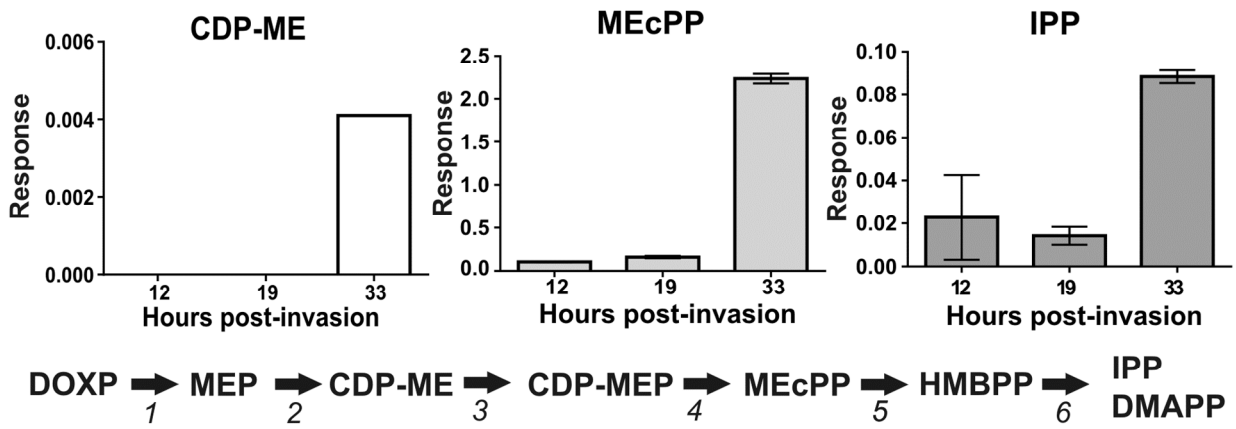

Figure 3. Highly synchronous parasites were recovered at different stages of *P. falciparum* intraerythrocytic cycle (12 hpi: rings, 19 hpi: trophozoites, 33 hpi: schizonts) and the presence of the MEP pathway intermediates was assessed by quantitative LC-MS/MS where only CDP-ME, MEcPP and IPP were detected. The levels of all three detected intermediates increased markedly between trophozoite (19 hpi) and schizont (33 hpi) stages. The response of each detected metabolite is expressed as the mean and S.E.M. of two biological replicates. *1*: 1-deoxy-D-xylulose-5-phosphate (DOXP) reductoisomerase, *2*: IspD, *3*: CDP-ME kinase, *4*: 2*C*-methyl-D-erythritol-2,4-cyclodiphosphate (MEcPP) synthase, *5*: 4-hydroxy-3-methyl-but-2-enyl pyrophosphate (HMBPP) synthase, *6*: HMBPP reductase.

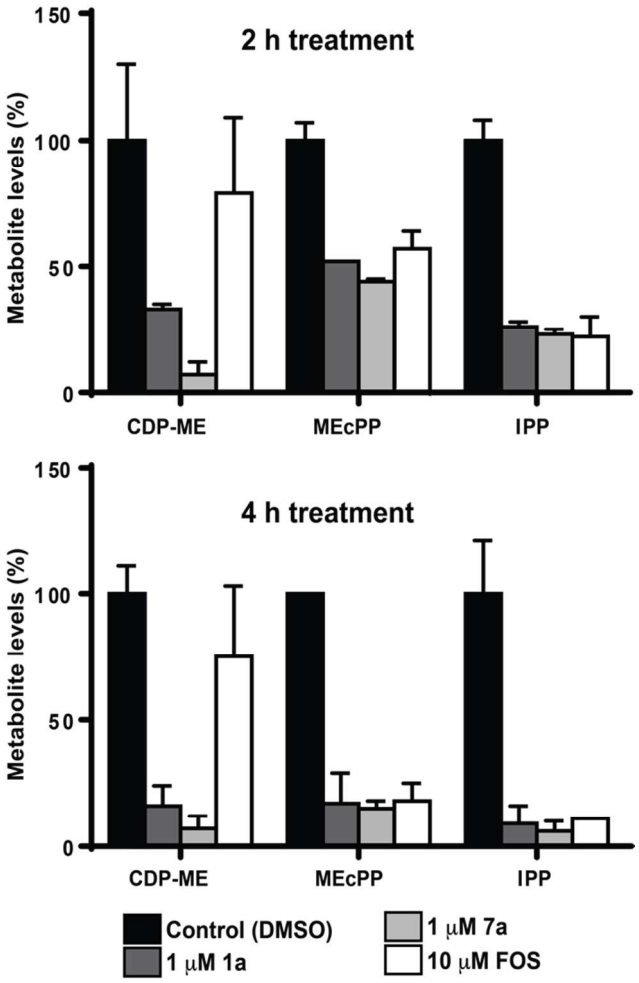

Figure 4. *In vivo* IspD inhibition assessed by quantitative LC-MS/MS. Highly synchronous schizont stage parasites were treated for 2 and 4 h with 1 μM **1a** or **7a**. FOS was used as positive control at 10 μM. After 2 h of drug exposure, **7a** caused a greater reduction on the cellular levels of the *Pf*IspD product CDP-ME than **1a**. The detected difference was statistically significant by the Benjamini-Hochberg significance test. Reduction of the cellular levels of the MEcPP and the final MEP pathway product, IPP, did not show significant differences among the three treatments after 2 h and 4 h of exposure to **1a**, **7a** and FOS as assessed by the Benjamini-Hochberg significance test. Results are expressed as a percentage of untreated control ± S.E.M. of two biological replicates.

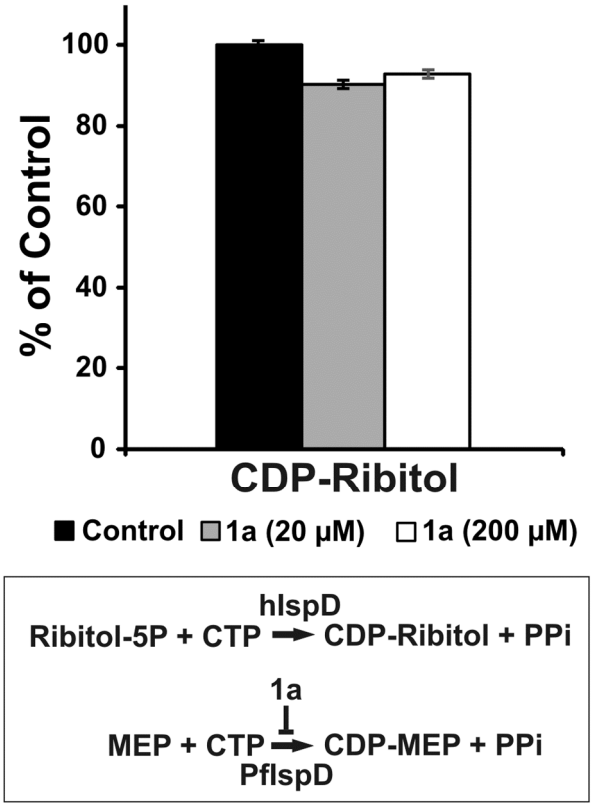

Figure 5. Human IspD is not targeted by **1a**. Human IspD enzymatic activity in the absence or presence of 20 and 200 μM of **1a** was measured by LC-MS/MS to monitor CDP-ribitol formation. The CDP-ribitol formation was not inhibited by the presence of **1a** at either concentration. The small reductions observed were not statistically significant by the Benjamini-Hochberg significance test. Mean ± S.E.M values were calculated from two independent assays.

For Table of Contents use only